

Indole-3-Lactic Acid Attenuates IMQ-Induced Psoriasiform Dermatitis in Mice via AhR-Dependent Suppression of IL-17A

Zhen Meng^{1,*}, Jieru Ren^{2,*}, Yuhsien Lai³, Siyao Lu², Huiyan Wu², Yanyun Jiang², Zhan Zhang⁴, Guozhen Tan², Zhenrui Shi²

¹Department of Dermatology, Guangzhou Dermatology Hospital, Guangzhou, Guangdong, People's Republic of China; ²Department of Dermatology, Sun Yat-sen Memorial Hospital, Sun Yat-sen University, Guangzhou, Guangdong, People's Republic of China; ³Department of Dermatology, The Eighth Affiliated Hospital, Sun Yat-sen University, Shenzhen, Guangdong, People's Republic of China; ⁴Center for Global Health, Nanjing Medical University, Nanjing, Jiangsu, People's Republic of China

*These authors contributed equally to this work

Correspondence: Zhenrui Shi, Department of Dermatology, Sun Yat-sen Memorial Hospital, Sun Yat-sen University, 107 Yanjiang West Road, Guangzhou, Guangdong, 510120, People's Republic of China, Tel +86 20 8133 2289, Email zrshi1989@outlook.com

Purpose: Psoriasis is a chronic immune-mediated skin disease increasingly linked to skin and gut dysbiosis. Microbiota-derived tryptophan catabolites act as endogenous ligands of the aryl hydrocarbon receptor (AhR) and modulate inflammation, but their role in psoriasis remains incompletely defined. Here, we aimed to determine whether the microbiota-derived tryptophan metabolite indole-3-lactic acid (ILA) modulates psoriasiform inflammation and to define its underlying mechanisms and therapeutic potential.

Methods: Using the imiquimod (IMQ)-induced mouse model of psoriasiform dermatitis (PsD), we profiled tryptophan metabolites by targeted LC-MS/MS in feces and serum. Mice received oral or topical ILA, with or without the AhR antagonist CH-223191. Ex vivo cervical lymph node (cLN) cells were stimulated with IL-23 + IL-1 β to assess IL-17A production by $\gamma\delta$ T cells. Separate cohorts received oral *Lactobacillus reuteri* supplementation. Public transcriptomic datasets were interrogated for cell type-specific AhR expression.

Results: Targeted metabolomics revealed reduced ILA levels in both feces and serum of IMQ-treated mice. Oral or topical ILA attenuated disease severity, reduced epidermal proliferation and neutrophil infiltration, and suppressed the expression of inflammatory transcripts, including Il17a. Notably, topical ILA was superior to benvitimod, a synthetic AhR agonist approved for the treatment of psoriasis, in suppressing IMQ-induced PsD. The AhR antagonist CH-223191 partially abrogated the protective effects of oral ILA. Ex vivo, ILA selectively suppressed IL-17A production by $\gamma\delta$ T cells, and this effect was reversed by AhR antagonism. *Lactobacillus reuteri* supplementation ameliorated PsD in an AhR-dependent manner, with fecal ILA levels inversely correlating with ear thickness and cutaneous neutrophil infiltration. Analysis of public datasets showed increased AhR expression in psoriatic T cells and a positive correlation of AhR and CYP1B1 with IL17A/IL17F.

Conclusion: These findings identify a microbiota-derived ILA-AhR axis that limits $\gamma\delta$ T17/IL-17-driven skin inflammation, and support metabolite supplementation or probiotic augmentation as potential therapeutic strategies for psoriasis.

Keywords: indole-3-lactic acid, psoriasis, aryl hydrocarbon receptor, IL-17A

Introduction

Psoriasis is a chronic, immune-mediated skin disease characterized by keratinocyte hyperproliferation and a feed-forward inflammatory loop between epidermal and immune cells. Central to its pathogenesis is the interleukin (IL)-23/IL-17 axis: IL-17A, primarily produced by T helper (Th) 17 cells and gamma delta ($\gamma\delta$) T cells, acts on keratinocytes to induce antimicrobial peptides (AMPs) and chemokines, thereby amplifying neutrophil recruitment and sustaining inflammation.¹

The pivotal role of IL-17A is underscored clinically by the robust efficacy of IL-17A/IL-17 receptor–blocking biologics, which rapidly improve lesions and normalize keratinocyte gene programs.²

Growing evidence indicates that gut dysbiosis contributes to the pathogenesis of psoriasis (PsO).³ Patients with PsO often exhibit altered microbial diversity and altered community composition. Gut dysbiosis not only disrupts gut barrier function and promotes microbial translocation and immune activation, but also reshapes the pool of bacteria-derived metabolites that modulate Th17/regulatory T cells (Treg) balance, cytokine production, and barrier integrity. Tryptophan (Trp), an essential amino acid, is metabolized by host cells via the kynurenine pathway or by intestinal microbes into indole derivatives.⁴ Indole derivatives are principal endogenous ligands for the aryl hydrocarbon receptor (AhR), a ligand-activated transcription factor expressed in immune and epithelial cells. Upon activation, AhR translocates to the nucleus and regulates downstream genes such as CYP1A1 and CYP1B1, as well as tight-junction proteins and AMPs.⁵ AhR signaling is essential for mucosal immune homeostasis by strengthening the epithelial barrier, promoting goblet-cell differentiation, and suppressing local inflammation. In murine models, indole derivatives or AhR agonists attenuated dextran sodium sulfate (DSS)-induced colitis.⁶ Consistently, reduced levels of AhR ligands and receptor expression have been reported in inflammatory bowel disease (IBD), a common comorbidity of psoriasis.⁷

Among microbial indoles, Indole-3-lactic acid (ILA) has emerged as a key immunoregulatory metabolite. ILA is produced by several gut commensals—notably *Lactobacillus* species such as *Lactobacillus reuteri* (*L. reuteri*)—and modulates T-cell differentiation and epithelial inflammation via AhR activation.^{8,9} For example, *L. reuteri* and ILA can reprogram intraepithelial CD4⁺ T cells toward CD4⁺CD8 $\alpha\alpha$ ⁺ regulatory phenotypes or suppress Th17 polarization, thereby dampening mucosal inflammation and preserving barrier integrity.¹⁰ While most studies have focused on the gut, whether the ILA-AhR axis exerts similar immunomodulatory effects in the skin, particularly in psoriasis, remains poorly understood.

In this work, we identify a protective role for microbiota-derived ILA in psoriasis. We show that ILA is decreased in mice with psoriasisform dermatitis (PsD) and that oral or topical ILA administration ameliorates imiquimod (IMQ)-induced PsD. Mechanistically, ILA acts through AhR activation to suppress IL-17A production by T cells. Moreover, supplementation with *L. reuteri*, a robust ILA producer, alleviates disease in an AhR-dependent manner. Together, these findings highlight the ILA-AhR pathway as a promising therapeutic axis in psoriasis.

Materials and Methods

Mouse Experiments

Animal ethics approval has been obtained for our study and all procedures conformed to the guidelines of the Institutional Animal Care and Use Committee (IACUC) of Sun Yat-sen University (SYSU-IACUC-2025-001861). Male and female C57BL/6 mice, 6–8 weeks old, were obtained from the Sun Yat-sen University Laboratory Animal Center (Guangzhou, China). Animals were housed under specific pathogen-free conditions in a climate-controlled facility (12-h light/dark cycle; HEPA-filtered fresh air; temperature and humidity regulated), with irradiated chow and water available ad libitum. Unless otherwise stated, five mice were maintained per cage.

To evaluate the effects of indole-3-lactic acid (ILA; MedChemExpress), mice received either oral gavage of ILA at 20 or 50 mg kg⁻¹ day⁻¹ in PBS (100 μ L per dose) beginning 2 days before imiquimod (IMQ) application and continuing through day 4. Topical ILA formulated in Vanicream at 0.5%, 1% or 2% (w/w), and Benvitimid (1%, w/w) was administered twice daily from day 0 to day 6. For probiotic intervention, *Lactobacillus reuteri* DSM17938 (BioGaia) was delivered by oral gavage at 1.0×10^8 CFU per day, starting 2 weeks prior to IMQ treatment and maintained throughout the experiment. Where indicated, the AhR antagonist CH-223191 (MedChemExpress) was given by intraperitoneal injection at 10 mg kg⁻¹ day⁻¹, commencing 2 days before and continuing during IMQ exposure.

Mice were randomly assigned to treatment arms. No additional measures were used to control potential confounders. Investigators responsible for administering treatments were aware of group allocation, whereas personnel performing clinical scoring, histopathology, and sample processing were blinded to treatment. No prespecified inclusion or exclusion criteria were applied. Formal power calculations were not performed; sample size was based on prior work and literature

precedents, using ear thickness as the primary outcome. Each in vivo experiment included biological replicates (and technical replicates where appropriate), as detailed in the figure legends, to support reproducibility.

Patient Samples

Lesional skin was obtained from patients with psoriasis vulgaris. Normal control skin was collected as perilesional tissue adjacent to excised benign nevi from age- and sex-matched healthy donors. The study protocol was approved by the Medical Ethics Committee of Sun Yat-sen Memorial Hospital, Sun Yat-sen University (approval No. SYSKY-2025-836-01). Written informed consent was obtained from all donors, and the study was conducted in accordance with the Declaration of Helsinki.

IMQ-Induced PsD Model

IMQ-induced PsD model was described previously.¹¹ 10 mg of 5% IMQ (Aldara; 3M Pharmaceuticals) in total was applied once daily to both sides of both ears for 5 consecutive days. For the assessment of ear skin inflammation severity, a Psoriasis Severity Index (PSI) scoring system was employed to evaluate the macroscopic clinical appearance of mice. The PSI scoring system was developed based on the clinical Psoriasis Area and Severity Index (PASI) and the extent of skin involvement in the determination of the overall score was excluded. Erythema, scaling, and thickening were independently scored on a scale from 0 to 4: 0, none; 1, slight; 2, moderate; 3, marked; 4, very marked. The cumulative daily score (with a maximum of 12) was determined for each animal. Ear thickness was measured daily using a Peacock G-1A dial thickness gauge (Ozaki MFG, Tokyo, Japan).

Flow Cytometry

The antibodies applied for staining included Anti-mouse $\gamma\delta$ -TCR (clone GL3), CD3 (17A2), IL17A (TC11-18H10.1), CD45 (30-F11), CD11b (M1/70), Ly6G (IA8) antibodies. The flow antibody details can be found in [Supplementary Table 1](#). Whole ear skin was minced and digested with liberase TM (Roche) and DNase I (Sigma-Aldrich) in RPMI1640 supplemented with 2% fetal bovine serum (FBS) at 37°C for 1 hour, aiming to yield complete skin cell suspensions before filtering the tissue through a 70 μ m cell strainer. Cervical draining lymph nodes were mechanically dissociated by gently pressing the tissue through a 70- μ m strainer in RPMI/2% FBS. Prior to staining, cells were incubated with anti-mouse CD16/32 (Fc γ RII/III, BD Biosciences) to block Fc-receptor-mediated binding. For intracellular cytokine assessment, cells were stimulated for 4–6 h with a cell activation cocktail (BioLegend), stained with surface antibodies, and then fixed and permeabilized using the eBioscience intracellular cytokine staining kit according to the manufacturer's instructions, followed by intracellular staining for IL-17A. Samples were acquired on a BD flow cytometer, and data were analyzed with FlowJo (BD Biosciences).

In vitro Experiments

HaCaT cells were obtained from DSMZ (German Collection of Microorganisms and Cell Cultures GmbH) and maintained in DMEM supplemented with 10% FBS, 10 U/mL of penicillin, and 10 μ g/mL of streptomycin. Cell line identity was confirmed by short tandem repeat (STR) profiling. Cells were stimulated with a cytokine comprising 50 ng/mL IL-17 and 10 ng/mL TNF- α in the absence or presence of 500 μ M ILA and 10 μ M CH-223191 (MedChemExpress) for 24 hours before following tests. Lymph node single-cell suspension (10⁶/mL) were planted 24-well plates with RPMI 1640 culture medium supplemented with 10% fetal bovine serum. After 12 to 24 hours incubation in the presence of IL-23 (50 ng/mL) and IL-1B (10 ng/mL) with ILA (500 μ M) and 10 μ M CH-223191 (MedChemExpress), cell were subject to following test.

Statistical Analysis

The presented data are expressed as mean \pm SEM. Statistical analyses were conducted using GraphPad Prism version 10 (GraphPad Software, San Diego, CA). A two-sided unpaired Student's *t*-test was employed for comparing two groups, while one-way analysis of variance (ANOVA) with with Dunnett's or Sidak's post hoc test was utilized for multiple

comparisons unless otherwise specified. Pearson correlation coefficient was utilized for correlation. A p-value less than 0.05 was deemed statistically significant.

Other experimental details are provided in the part of [Supplementary Methods](#).

Results

PsD is Associated with Reduced ILA in Feces and Serum

We conducted *in vivo* experiments using a mouse model of IMQ-induced PsD and profiled tryptophan-derived metabolites in feces from IMQ-treated mice versus vehicle (Vanicecream) controls using targeted liquid chromatography-tandem mass spectrometry (LC-MS/MS). Most differentially abundant features clustered within indole and indole-derivative pathways (Figure 1A). Among them, ILA showed a marked reduction in IMQ mice (log₂ fold change = -2.14), ranking second among the decreased indole metabolites (Figure 1B). Other common indole derivatives including indole, indoleacetate, Indole-3-acetic acid (IAA), and Indole-3-propionic acid (IPA) were also declined in feces, albeit to a lesser extent (Figure 1C). In serum, tryptophan and ILA were lower in IMQ mice, whereas IPA and IAA were increased (Figure 1D and E). We further assessed skin levels of tryptophan-route metabolites in mice and humans. Although most indole derivatives were below the limit of detection (likely reflecting low tissue abundance and limited sample size), tryptophan was significantly reduced in psoriatic lesional skin compared with healthy skin (Figure 1F). Collectively,

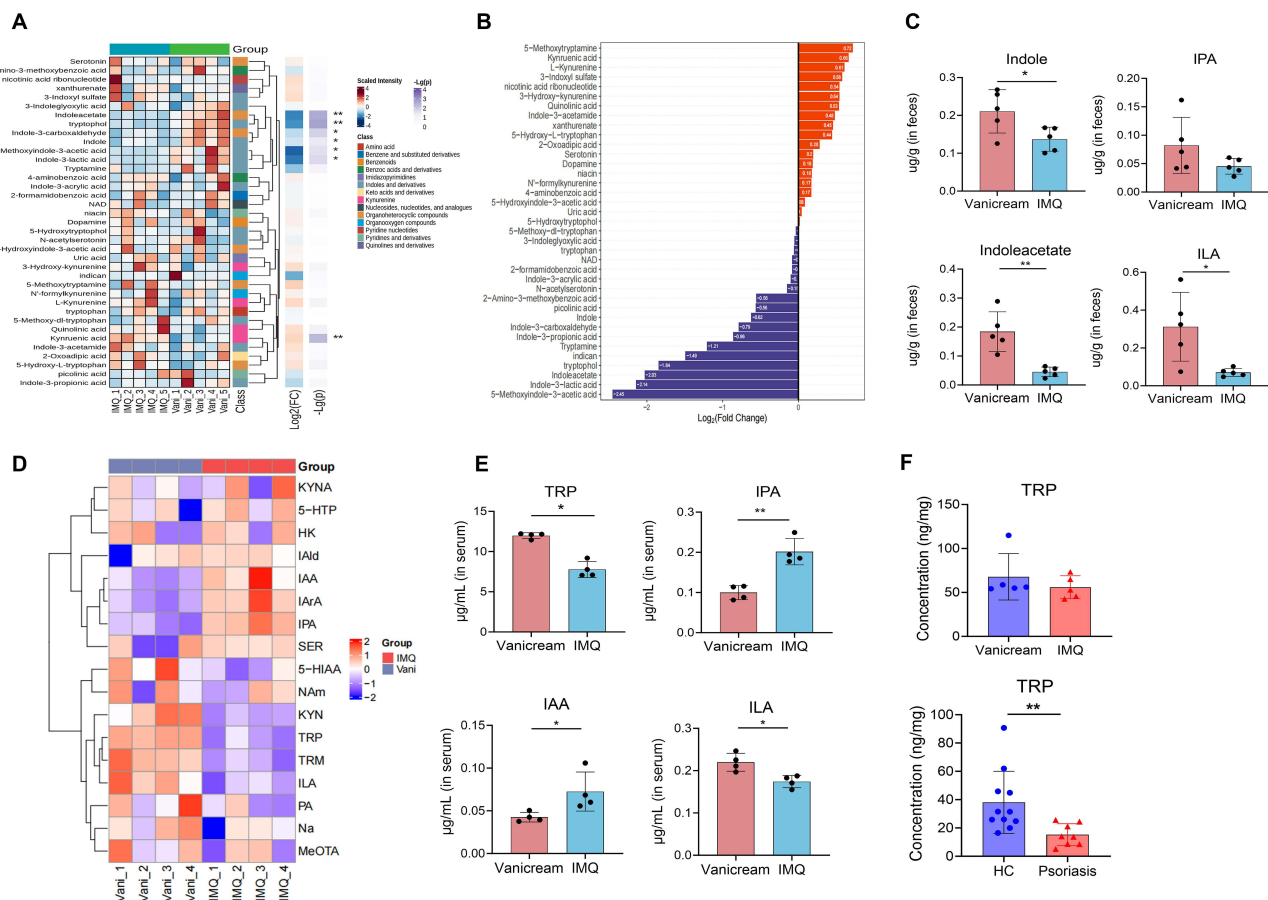


Figure 1 Tryptophan-derived metabolites in IMQ-induced psoriasisform dermatitis (PsD). **(A)** Targeted LC-MS/MS of fecal metabolites from IMQ-treated mice and Vanicecream-treated controls (Vani). Heat map shows z-scored intensities per sample. **(B)** Rank plot of fecal metabolites ordered by log₂(fold-change) (IMQ vs Vani). Orange bars indicate higher values in IMQ; purple bars indicate lower values in IMQ. **(C)** Fecal validation plots for selected indole-related metabolites: indole, indole-3-propionic acid (IPA), indoleacetate, and indole-3-lactic acid (ILA). **(D)** Heat map of serum metabolites measured by targeted LC-MS/MS in the same cohorts. **(E)** Serum validation plots for tryptophan (TRP), IPA, indole-3-acetic acid (IAA), and ILA. Bars indicate group means with individual values overlaid. **(F)** Skin measurements of tryptophan. Top: mouse skin (Vani vs IMQ). Bottom: human skin (healthy controls vs psoriasis lesional skin). **(C, E and F)** data are presented as mean ± SEM. *p < 0.05, **p < 0.01.

these data indicate disrupted tryptophan-indole metabolism in IMQ-induced PsD, with ILA consistently decreased in both feces and serum.

Oral Administration of ILA Attenuates PsD in Mice

We evaluated whether ILA modulates psoriatic inflammation using the IMQ-induced PsD model. Mice were orally administered vehicle, a low dose of ILA (20 mg/kg/day), or a high dose of ILA (50 mg/kg/day) via daily gavage starting 2 days prior to IMQ application and continuing through day 4 (Figure 2A). Body weight was comparable across groups over the dosing period (data not shown). ILA treatment significantly reduced erythema, scaling, and ear thickness, resulting in lower Psoriasis Severity Index (PSI) scores (Figure 2B). No significant differences were observed between the low- and high-dose ILA groups. Histological analysis confirmed that ILA treatment reduced epidermal thickness and the number of Munro microabscesses (Figure 2C). Immunohistochemistry (IHC) revealed decreased nuclear Ki-67 staining in the epidermis of ILA-treated mice, indicating reduced keratinocyte proliferation (Figure 2D). IHC staining also showed reduced infiltration of CD3+ T cells in the skin of ILA-treated mice compared with vehicle-treated controls (Supplementary Figure 1). Oral treatment of ILA had no apparent effect on spleen index or total cellularity of skin-draining cervical lymph nodes (cLNs) (Figure 2E). Flow cytometric analysis demonstrated reduced neutrophil infiltration in the ear skin of ILA-treated mice, with statistical significance observed in the high-dose group compared to vehicle controls (Figure 2F). Furthermore, quantitative PCR analysis showed that ILA treatment suppressed mRNA expression

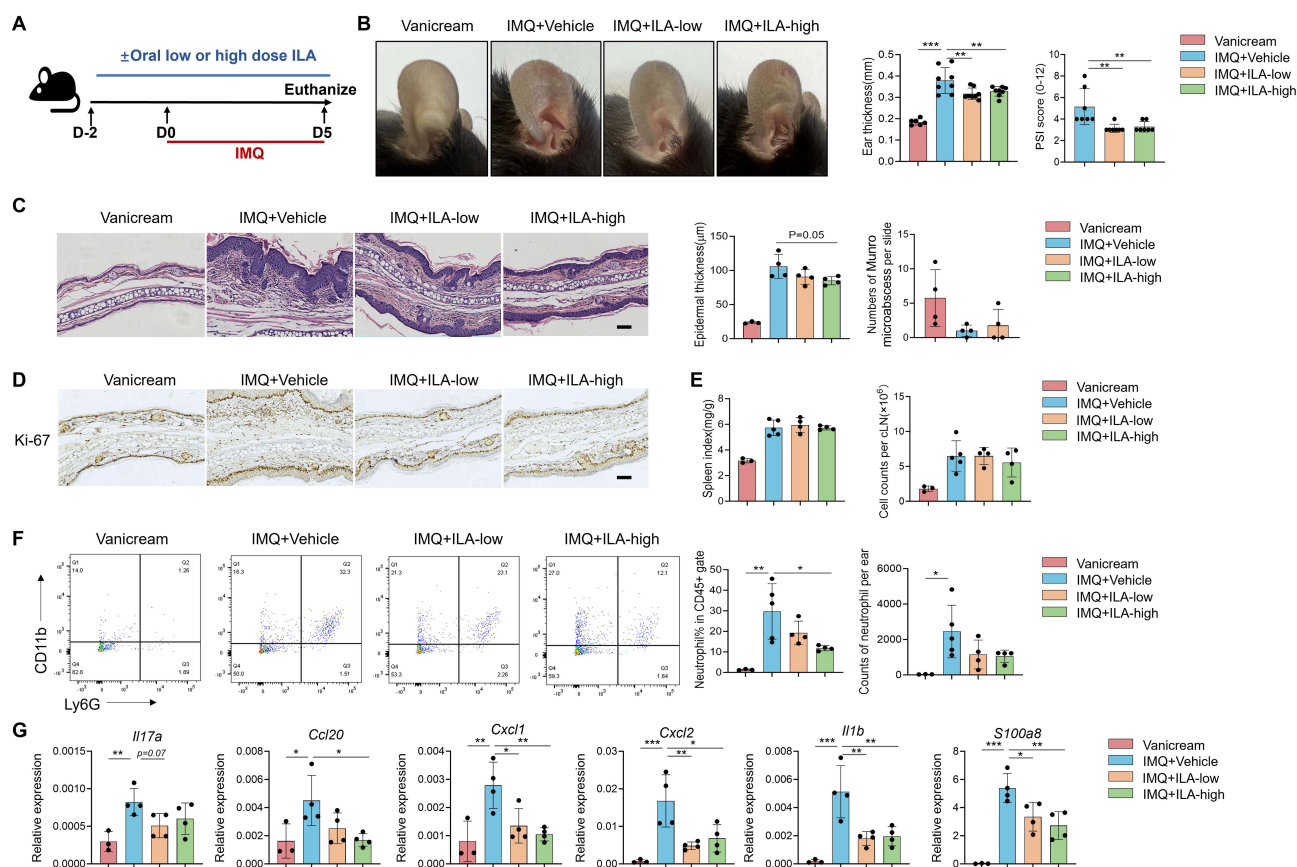


Figure 2 Oral supplementation of ILA ameliorates PsD in mice. (A) Schematic of the experimental design. Mice received daily oral gavage of vehicle, ILA-low (20 mg/kg), or ILA-high (50 mg/kg) beginning 2 days prior to IMQ and continuing through day 4. Tissues were harvested on day 5. Topical IMQ was applied to induce PsD. Vanicream served as vehicle control. (B) Representative ear photographs, ear thickness and Psoriasis Severity Index (PSI) from each group on day 5. (C) Representative H&E-stained ear sections. Quantification of epidermal thickness and Munro microabscess counts. (D) Representative Ki-67 IHC of epidermis. (E) Spleen index and total cell counts per skin-draining cervical lymph nodes (cLNs). (F) Representative flow-cytometry plots of ear single-cell suspensions, neutrophils were defined as CD11b⁺Ly6G⁺ in CD45⁺ gate. Quantification of percentage and absolute counts of neutrophils per ear. (G) RT-PCR measurements of psoriasis-associated transcripts in ear tissue. Scale bars: (C and D), 100 µm. Data are presented as mean ± SEM, with each dot representing one mouse. Statistical tests for multi-group comparisons were performed by one-way ANOVA with Dunnett's test compared to IMQ+vehicle group. *p < 0.05, **p < 0.01, ***p < 0.001.

of psoriasis-associated inflammatory mediators, including *Il17a*, *Ccl20*, *Cxcl1*, *Cxcl2*, *Il1b*, and *S100a8* (Figure 2G). Taken together, these findings demonstrate that oral ILA administration effectively mitigates IMQ-induced PsD in mice.

Topical Administration of ILA Ameliorates PsD

We next investigated whether topical application of ILA could confer similar anti-psoriatic effects as oral delivery. To this end, IMQ-treated mice received topical administration of 0.5% or 2% (w/w) ILA formulated in Vanicream, applied twice daily (Figure 3A). No weight loss or other adverse effects were observed in the ILA-treated groups during the study period (data not shown). Similar to oral administration, topical ILA significantly improved erythema, reduced ear swelling and PSI in IMQ-treated mice with similar responses at 0.5% and 2% (Figure 3B and C). Histology showed reduced

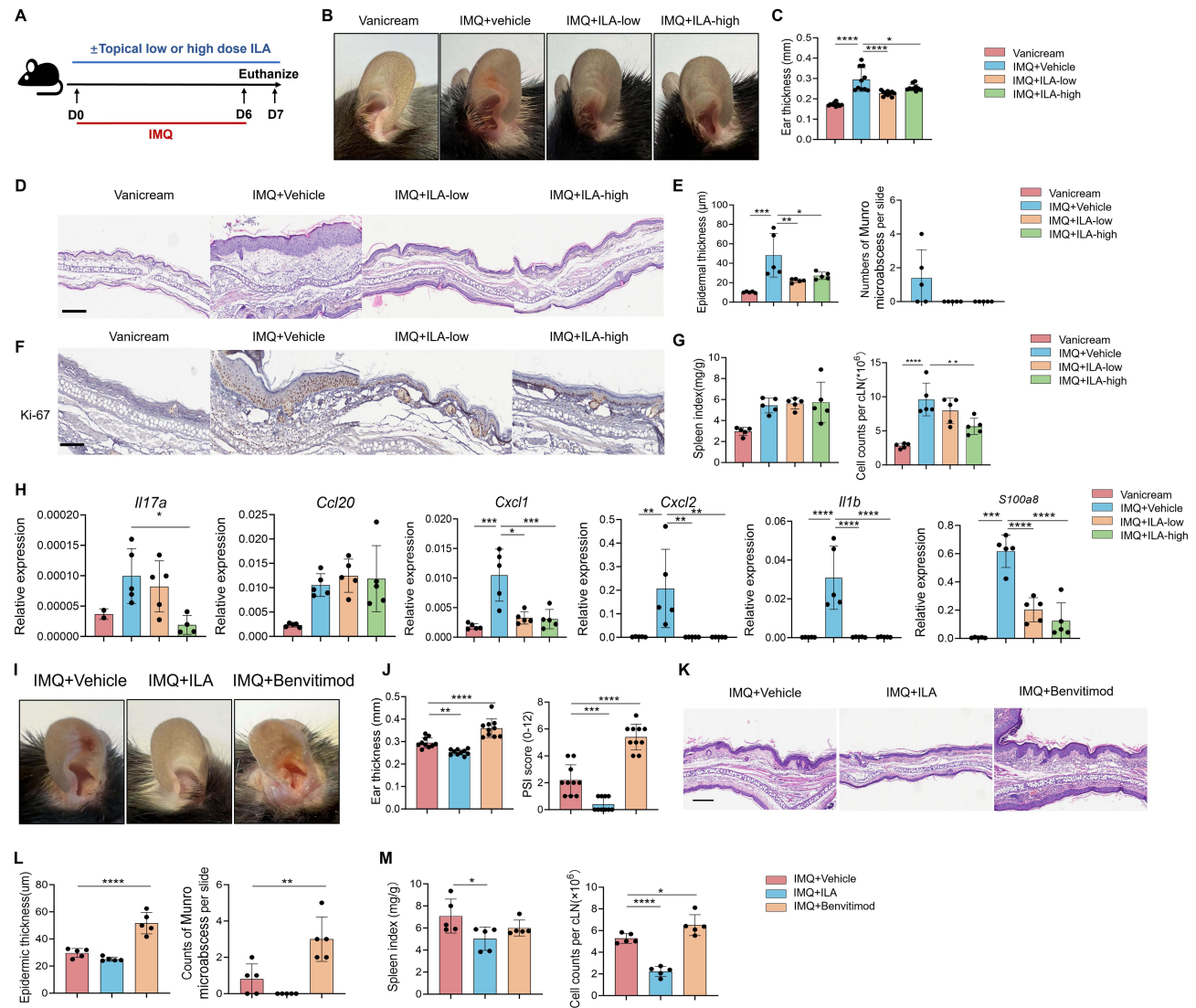


Figure 3 Topical application of ILA ameliorate PsD in mice. **(A)** Schematic of the experimental design. Mice received topical iniquimod (IMQ) on the ears and were treated with vehicle (Vanicream), low-dose ILA (0.5% w/w), or high-dose ILA (2% w/w) formulated in Vanicream, applied twice daily from day 0 to day 6; ear tissues were collected on day 7. **(B)** Representative ear photographs from each group at endpoint. **(C)** Ear thickness and Psoriasis Severity Index (PSI). **(D)** Representative H&E-stained ear sections. **(E)** Quantification of epidermal thickness and Munro microabscesses per section. **(F)** Representative Ki-67 IHC of the epidermis. **(G)** Spleen index and total cell counts in cervical skin-draining lymph nodes (cLNs). **(H)** RT-PCR measurements of psoriasis-associated transcripts in ear tissue. **(I-M)** mice received topical IMQ on the ears and were treated with vehicle, ILA (1% w/w) formulated in Vanicream, or benvitimid (1%), applied twice daily from day 0 to day 6, ear tissues were collected on day 7. **(I)** Representative ear photographs from each group at endpoint. **(J)** Ear thickness and PSI. **(K)** Representative H&E-stained ear sections. **(L)** Quantification of epidermal thickness and Munro microabscesses per section. **(M)** Spleen index and total cell counts in cLNs. Data are presented as mean \pm SEM, with each dot representing one mouse. Scale bars: **(D and K)**, 200 μ m; **F**, 100 μ m. Statistical tests for multi-group comparisons were performed by one-way ANOVA with Dunnett's post hoc test versus the IMQ + vehicle group. * $p < 0.05$, ** $p < 0.01$, *** $p < 0.001$, **** $p < 0.0001$.

epidermal thickness and a trend toward fewer Munro microabscesses in ILA-treated ears (Figure 3D and E). IHC indicated reduced epidermal proliferation and decreased infiltration of CD3⁺ T cells (Figure 3F, [Supplementary Figure 2](#)). Topical ILA did not alter IMQ-associated splenomegaly, whereas the 2% formulation was associated with lower total cellularity in cLNs (Figure 3G). At the transcriptional level, PCR demonstrated decreased mRNA abundance of *Il17a*, *Cxcl1*, *Cxcl2*, *Il1b*, and *S100a8* in ILA-treated tissue (Figure 3H).

Benvitimod is an aryl hydrocarbon receptor (AhR) agonist approved for the treatment of plaque psoriasis. We next compared the anti-psoriatic efficacy of topical ILA and benvitimod. Unexpectedly, the commercial benvitimod ointment aggravated IMQ-induced PsD in our experimental setting, likely reflecting irritant effects of the formulation. In contrast, topical ILA at the same concentration ameliorated skin inflammation, as evidenced by reduced erythema (Figure 3I), decreased ear thickness, and lower PSI scores (Figure 3J). Histologically, ILA-treated mice showed a trend toward reduced epidermal thickness and fewer Munro microabscesses (Figure 3K and L). Additionally, ILA inhibited IMQ-associated splenomegaly and reduced cellularity in cLNs compared with vehicle-treated controls (Figure 3M). In mice treated topically with benvitimod ointment alone, we observed visible ear swelling and erythema, along with a reduced spleen index, suggesting a possible local irritant effect of the formulation under these conditions ([Supplementary Figure 3](#)). These findings are limited to the acute IMQ model and should not be directly extrapolated to human psoriasis, particularly chronic lesions.

Collectively, under the conditions tested, topical ILA attenuated IMQ-induced PsD and was associated with reduced keratinocyte proliferation and inflammatory gene expression.

Oral Treatment of ILA Inhibits PsD Through AhR

ILA has been shown to regulate both physiological and pathological processes, primarily through its ability to bind and activate the AhR.⁸ To test whether AhR signaling underlies ILA's effects in PsD, mice received daily oral ILA beginning 2 days before IMQ application, with concurrent daily intraperitoneal injection of CH-223191 (AhR antagonist) or vehicle (Figure 4A). AhR inhibition aggravated disease phenotype including erythema, scaling, ear thickness, and the PSI were all higher with CH-223191 than with vehicle (Figure 4B). Histology showed greater epidermal thickness and more Munro microabscesses (Figure 4C and D), and Ki-67 iIHC revealed increased epidermal proliferative activity (Figure 4E). Systemic indices were also affected: spleen index and total cellularity of cLNs increased with CH-223191 (Figure 4F). By flow cytometry, CH-223191 promoted accumulation of IL-17A-producing CD3⁺ T cells and $\gamma\delta$ T cells in cLNs (Figure 4G) and elevated both the frequency and absolute number of neutrophils in ear skin from ILA-fed, IMQ-treated mice (Figure 4H). Consistent with these findings, qPCR showed higher *Il17a*, *Il1b*, *Cxcl1*, and *Cxcl2* mRNA in skin after CH-223191 treatment (Figure 4I). We compared IMQ+vehicle versus IMQ + CH-223191 mice and found no significant differences in clinical appearance, histopathology, or molecular readouts ([Supplementary Figure 4](#)), indicating that, under AhR inhibitor alone did not exacerbate IMQ-induced PsD. Together, these data indicate that the anti-psoriatic activity of oral ILA is dependent, at least in part, on AhR, as pharmacologic AhR blockade abrogated ILA-associated improvements and exacerbated inflammation.

ILA Suppresses IL-17A Production by $\gamma\delta$ T Cells via AhR Signaling

In vivo, ILA ameliorated PsD concomitant with reduced cutaneous IL-17A. Given the central role of this cytokine, we tested whether ILA constrains IL-17A production by T cells. Because $\gamma\delta$ T cells are the predominant IL-17A source in murine PsD, cLN cells were stimulated ex vivo with IL-23 and IL-1 β to favor $\gamma\delta$ T17 activation rather than conventional Th17 polarization.¹² After 12 h, *Il17a* transcripts were markedly reduced by ILA, and this effect was abrogated by the AhR antagonist CH-223191 (Figure 5A). Flow cytometry corroborated these findings: ILA decreased the frequency of IL-17A⁺ $\gamma\delta$ T cells and lowered total IL-17A fluorescence per sample, with minimal change in IL-17A mean fluorescence intensity (MFI) (Figure 5B and C). CH-223191 alone had little impact but substantially reversed ILA-mediated suppression, most prominently in the $\gamma\delta$ T-cell compartment. Together, these data indicate that ILA restrains IL-17A production by T cells, particularly $\gamma\delta$ T cells, via AhR-dependent mechanisms.

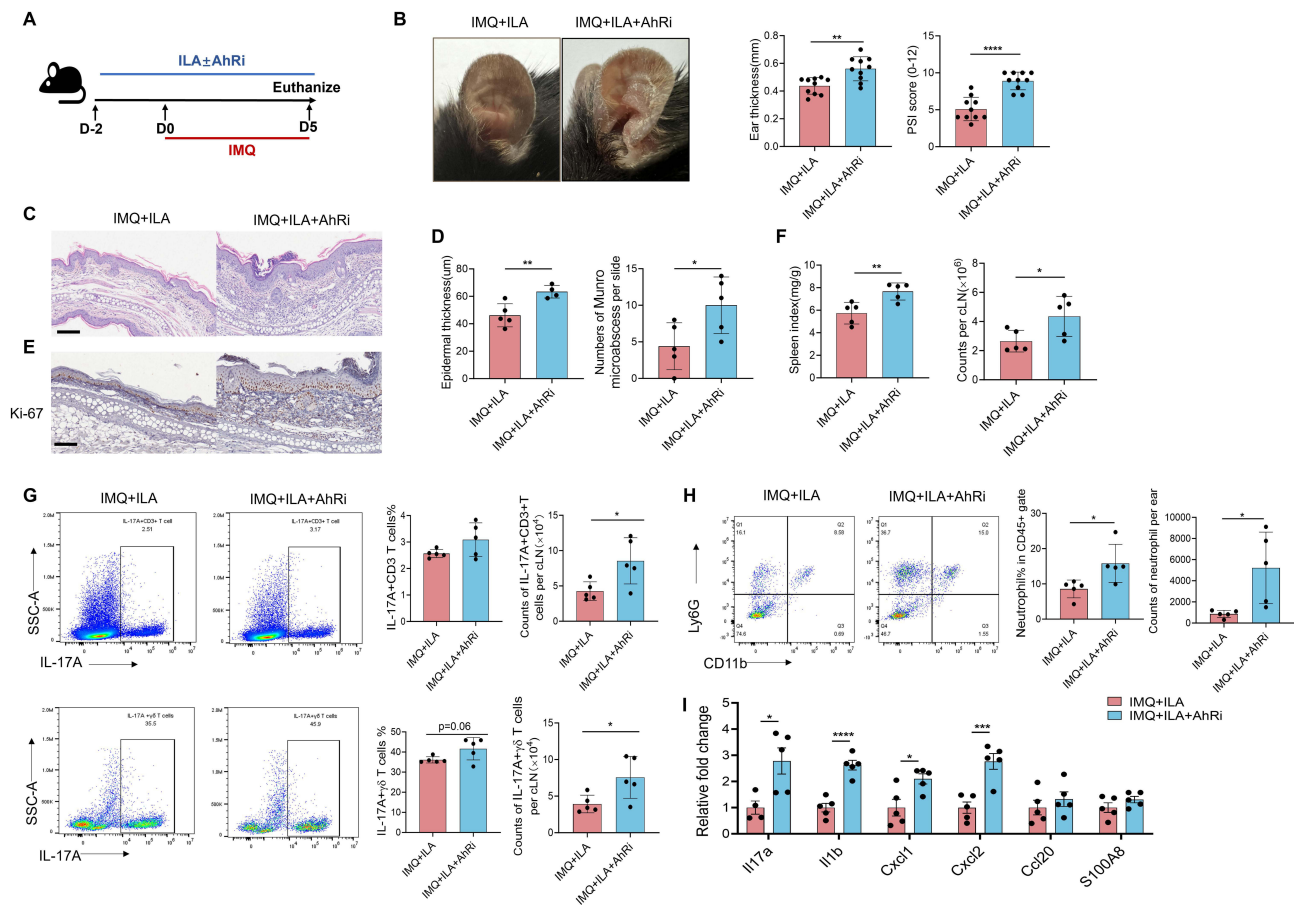


Figure 4 Pharmacologic AhR inhibition counteracts the effects of oral ILA in IMQ-induced PsD. **(A)** Experimental scheme. Mice received daily oral ILA beginning day -2 relative to IMQ application. A subset was co-treated with the AhR antagonist CH-223191 (AhRi) by daily intraperitoneal injection. Tissues were collected on day 5. **(B)** Representative ear photographs, ear thickness and Psoriasis Severity Index (PSI) at endpoint. **(C)** Representative H&E-stained ear sections. **(D)** Quantification of epidermal thickness and Munro microabscesses per section. **(E)** Representative Ki-67 IHC of epidermis. Scale bars, $100\mu\text{m}$. **(F)** Spleen index and total cellularity of cervical skin-draining lymph nodes (cLNs). **(G)** Flow-cytometry analysis of cLNs. Left: representative plots; right: frequencies of IL-17A⁺ CD3⁺ T cells in CD3⁺ gate and IL-17A⁺ $\gamma\delta$ T cells in TCR $\gamma\delta$ ⁺ gate. **(H)** Neutrophils in ear skin. Left: representative plots (neutrophils defined as CD11b⁺Ly6G⁺); right: frequency within live CD45⁺ cells and absolute counts per ear. **(I)** RT-PCR of ear tissue showing relative mRNA levels of psoriasis-associated genes. Scale bars: C and E, $100\mu\text{m}$. Data are presented as mean \pm SEM, with each dot representing one mouse. Statistical comparisons between two groups used two-tailed unpaired t-tests. * $p < 0.05$, ** $p < 0.01$, *** $p < 0.001$, **** $p < 0.0001$.

ILA Suppresses Keratinocyte Inflammation with Limited Involvement of AhR

We examined whether ILA modulates keratinocyte inflammatory responses. HaCaT cells were co-stimulated with IL-17A and TNF- α ,¹³ which increased transcripts for chemokines (CCL20, CXCL1, CXCL2), antimicrobial peptides (S100A7, S100A8), and cytokines (IL1B, IL6). ILA broadly attenuated these inductions while effects on IL1B were minimal (Figure 6A). Blocking AhR with CH-223191 produced only modest attenuation of ILA's inhibition and chiefly for S100A7/A8, with little to no impact on CCL20, CXCL1/CXCL2, or IL6 (Figure 6B). Thus, under these conditions and doses, ILA's anti-inflammatory effects in keratinocytes appear largely AhR-independent, with at most a minor AhR contribution to a subset of readouts.

L. reuteri Ameliorates PsD Through AhR

We tested whether *L. reuteri*, a robust producer of ILA, mitigates IMQ-induced PsD and whether this effect involves AhR signaling. Mice were fed *L. reuteri* daily for 2 weeks before IMQ application and treatment continued throughout the experiment (Figure 7A). Relative to vehicle, *L. reuteri* reduced erythema, scaling, and ear swelling, resulting in lower PSI scores (Figure 7B). Histology showed decreased epidermal thickness and fewer Munro microabscesses in the *L. reuteri* group (Figure 7C). *L. reuteri* also attenuated IMQ-associated splenomegaly (Figure 7D). Consistent with reduced microabscess formation, neutrophil frequency and absolute counts in ear skin were lower after *L. reuteri*

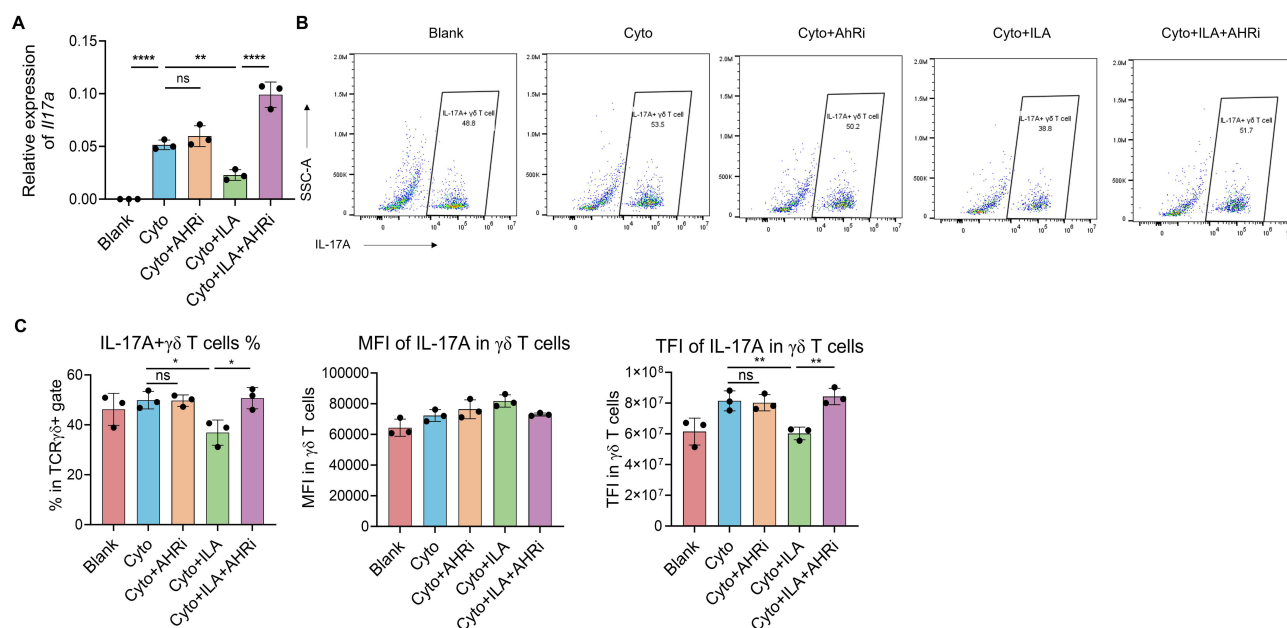


Figure 5 ILA inhibits IL-17A production by $\gamma\delta$ T cell in vitro. **(A)** *Il17a* mRNA in cervical lymph node (cLN) cells after 12 h stimulation with IL-23 (50 ng/mL) + IL-1 β (10 ng/mL) (Cyto) in the absence or presence of indole-3-lactic acid (ILA) and/or the AhR antagonist CH-223191 (AhRi). **(B)** Representative intracellular cytokine staining plots showing IL-17A-producing $\gamma\delta$ T cells within the CD3⁺ TCR $\gamma\delta$ ⁺ gate after 24 h under the indicated conditions. **(C)** Quantification of (left) the frequency (%) of IL-17A⁺ $\gamma\delta$ T cells, (middle) mean fluorescence intensity (MFI) of IL-17A within IL-17A⁺ $\gamma\delta$ T cells, and (right) total fluorescence intensity (TFI) of IL-17A across the $\gamma\delta$ T-cell gate (sum signal per sample). Bars show mean \pm SEM with individual data points (each dot = one biological replicate). Group comparisons used one-way ANOVA with Šidák post hoc tests; ns, not significant; *, P < 0.05; **, P < 0.01; ****p < 0.0001.

treatment (Figure 7E). Notably, fecal ILA concentrations correlated inversely with PSI and neutrophil percentages, linking protective effect of *L. reuteri* to ILA production (Figure 7F).

To assess AhR dependence, mice received daily oral *L. reuteri* beginning 2 weeks before IMQ and were co-treated with the AhR antagonist CH-223191 or vehicle starting 2 days before IMQ (Figure 7G). AhR inhibition counteracted the benefits of *L. reuteri*, as evidenced by greater erythema, scaling, ear swelling, and higher PSI scores in the *L. reuteri* + AhRi group (Figure 7H). Histological analyses revealed increased Munro microabscesses with AhR blockade while there was no significant difference regarding epidermal thickness (Figure 7I and J). These findings indicate that *L. reuteri* improves PsD through AhR activation, likely mediated by microbially derived ILA.

AhR Expression is Altered in Psoriatic Skin and Correlates with IL-17A Expression

We examined the expression of AhR and its downstream mediators (CYP1A1, CYP1B1, and AHRR) in psoriatic lesions versus healthy controls using publicly available transcriptomic datasets. Consistent with prior reports, AhR abundance was reduced in psoriatic lesions compared with normal skin and was partially restored following biologic therapy (Figure 8A). At the cellular level, expression patterns differed among subsets (Figure 8B): in keratinocytes, AhR expression was diminished in psoriatic lesions and remained low after treatment; in endothelial cells, AhR was decreased in lesions but recovered to normal levels after therapy; in T cells, however, AhR expression was increased in psoriatic lesions and declined after treatment. These findings suggest that AhR plays divergent roles across distinct cell types within psoriatic skin. In T cells, AhR and CYP1B1 expression correlated positively with IL-17A expression (Figure 8C), linking AhR activity to the pathogenic IL-17 axis in psoriasis. Collectively, these observations indicate that AhR expression is dynamically regulated in psoriasis and may contribute to IL-17-driven inflammation in T cells.

Discussion

Several studies support a role for microbiota-derived tryptophan metabolites in restraining psoriasiform inflammation through AhR signaling. Consistent with earlier work showing that AhR activation dampens psoriatic inflammation whereas AhR deficiency exacerbates IMQ-induced dermatitis,¹⁴ a recent keratinocyte-focused study showed that ILA

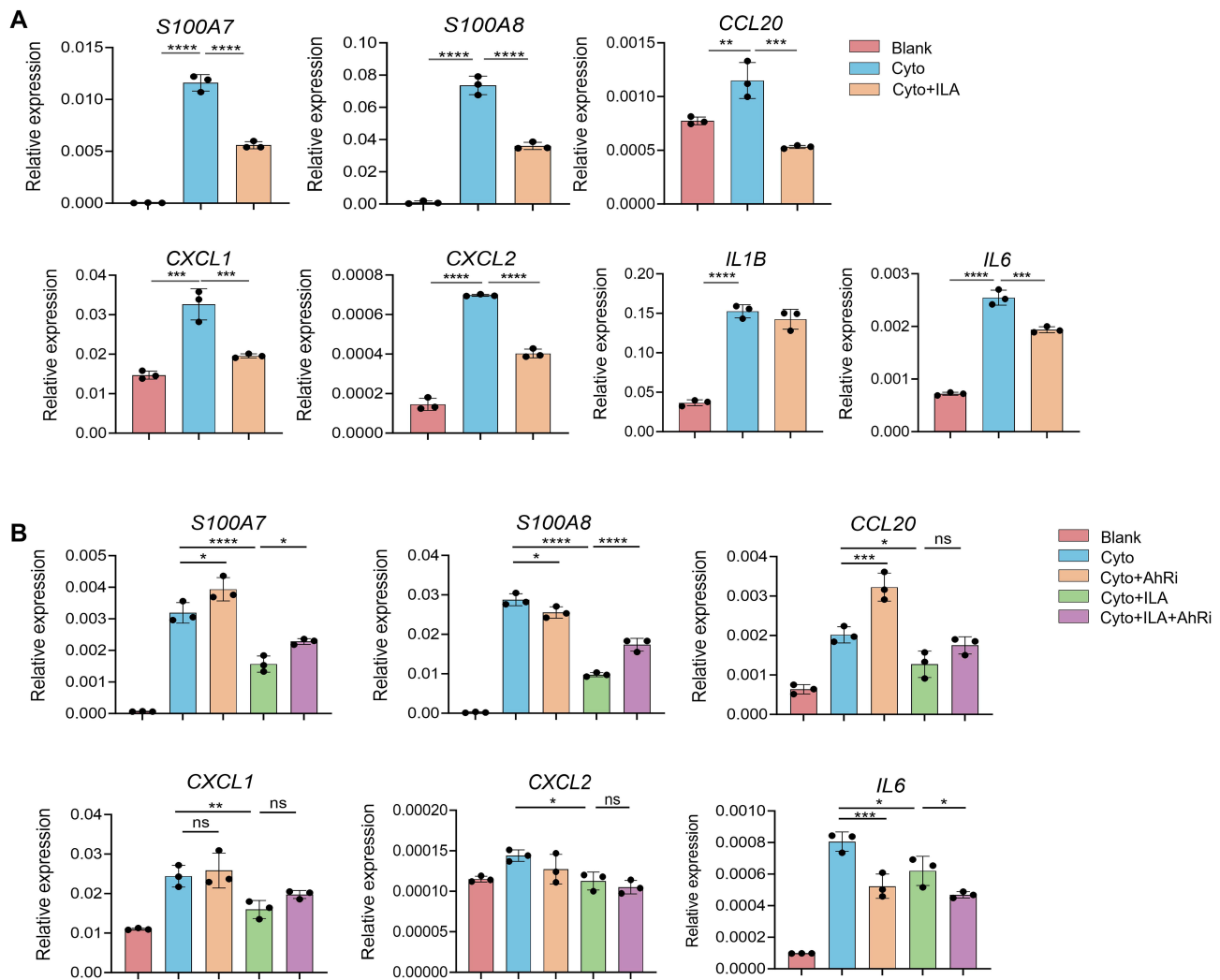


Figure 6 ILA inhibits inflammation of keratinocytes with limited involvement of AhR. **(A)** HaCaT cells were stimulated with IL-17A + TNF- α (Cyto) in the presence or absence of ILA. Relative mRNA abundance of S100A7, S100A8, CCL20, CXCL1, CXCL2, IL1B, and IL6 is shown. **(B)** Effect of AhR antagonism: Cells were treated with cytokines plus AhR inhibitor CH-223191 (AhRi) and/or ILA. In the presence of ILA, CH-223191 produced an observable upward shift for S100A7 and S100A8 compared with cytokines + ILA, with minimal change for CCL20, CXCL1, CXCL2, and IL6 under the same comparison. Data are presented as mean \pm SEM, with each dot representing one biological replicate. **(A)** statistical tests for multi-group comparisons were performed by one-way ANOVA with Dunnett's test compared to Cyto group, **(B)** statistical tests for multi-group comparisons were performed by one-way ANOVA with Sidak's test comparing selected groups. * $p < 0.05$, ** $p < 0.01$, *** $p < 0.001$, **** $p < 0.0001$. ns, not significant.

suppresses epidermal hyperproliferation in an AhR-dependent manner.¹⁵ In parallel, *L. reuteri* supplementation was reported to ameliorate IMQ-induced psoriasis-like inflammation and reduce Th17-associated responses.¹⁶ More recently, a strain-resolved *Limosilactobacillus reuteri* study further showed AhR-dependent protection through regulation of the IL-1 β /IL-17A axis and identified certain indole derivatives among major AhR-active metabolites.¹⁷

Here, we extend this framework by positioning ILA within a gut–skin metabolic–immune axis. We show that ILA is selectively reduced in both feces and serum in psoriasisform mice, suggesting cross-compartment disruption of tryptophan–indole metabolism during disease. Both oral and topical ILA ameliorated IMQ-induced skin inflammation across clinical, histologic, and transcriptional readouts, and we further compared the efficacy of topical ILA with benvitimod. Mechanistically, pharmacologic antagonism supported AhR dependence, and ILA suppressed IL-17A production by $\gamma\delta$ T cells, linking ILA–AhR signaling to the IL-23/IL-17 axis. Finally, a microbiome-based intervention showed that *L. reuteri*, a robust ILA producer, restored fecal ILA levels and mitigated disease in an AhR-dependent manner.

Previous studies have attributed anti-inflammatory actions to ILA, for example, AhR-dependent reductions in IL-8 production by intestinal epithelial cells.^{18,19} Consistent with prior studies, we found that ILA reduced cytokine-induced

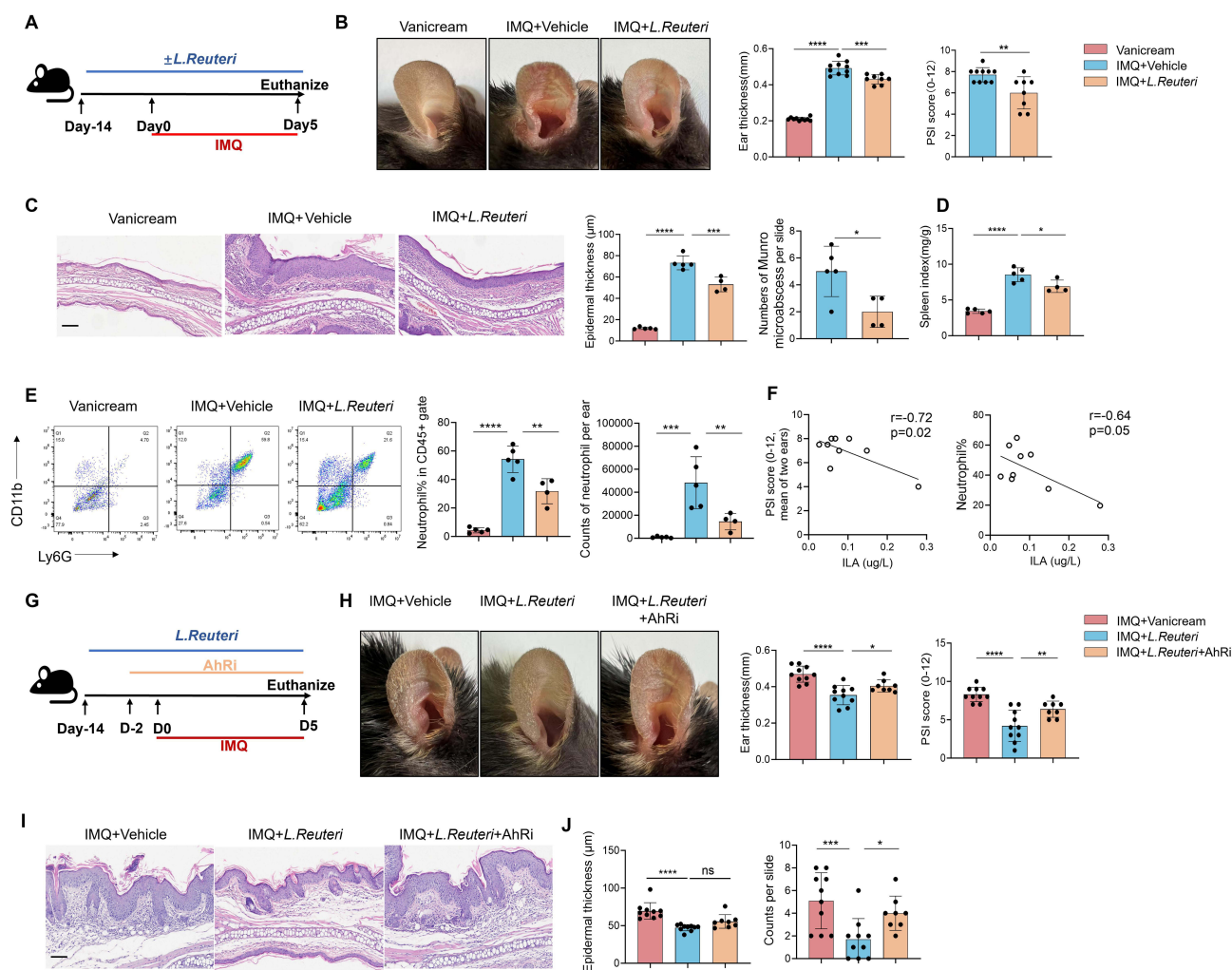


Figure 7 *Lactobacillus reuteri* mitigates IMQ-induced PsD and requires AhR signaling. **(A)** Experimental scheme for oral *L. reuteri* treatment. Mice received daily *L. reuteri* beginning day -14 and throughout IMQ treatment, tissues were collected on day 5. **(B)** Representative ear photographs, ear thickness and Psoriasis Severity Index (PSI) at endpoint. **(C)** Representative H&E-stained ear sections. Quantification of epidermal thickness and Munro microabscesses per section. **(D)** Spleen index at endpoint. **(E)** Representative flow-cytometry plots of ear single-cell suspensions, neutrophils were defined as CD11b⁺Ly6G⁺ in CD45⁺ gate. Quantification of percentage and absolute counts of neutrophils per ear. **(F)** Correlation of fecal ILA concentration with ear thickness (left) and neutrophil frequency in ear skin (right) from IMQ-treated mice receiving vehicle or *L. reuteri*. Lines indicate linear fit with Pearson r and p values. **(G)** Experimental scheme for AhR blockade during *L. reuteri* treatment. Mice received daily oral *L. reuteri* starting day -14 and were co-treated with CH-223191 (AhRi) or vehicle beginning day -2, tissues were collected on day 5. **(H)** Representative ear photographs, ear thickness and PSI. **(I)** Representative H&E-stained ear sections and **(J)** quantification of epidermal thickness and Munro microabscesses. Scale bars: C and I, 100 μm . Data are presented as mean \pm SEM. Statistical comparisons between two groups used two-tailed unpaired t-tests, statistical tests for multi-group comparisons were performed by one-way ANOVA with Dunnett's test compared to IMQ+vehicle group. Pearson correlation coefficient was utilized for correlation. * $p < 0.05$, ** $p < 0.01$, *** $p < 0.001$, **** $p < 0.0001$, ns, not significant.

pro-inflammatory transcripts in keratinocytes, with only limited AhR dependence under our experimental conditions. This divergence likely reflects cell type- and context-specific signaling: our ex vivo data support AhR-linked ILA activity in $\gamma\delta$ T cells, whereas keratinocytes may also engage alternative pathways. Consistent with this view, analysis of a public dataset showed that AhR is reduced in keratinocytes and endothelial cells but increased in T cells in psoriatic skin. This compartment-specific pattern likely suggests an imbalance in AhR biology across epithelial, vascular, and immune compartments. Reduced AhR expression in keratinocytes and endothelial cells may indicate loss of tissue-protective homeostatic signaling, in line with reports that AhR activation suppresses psoriasiform inflammation and that endothelial AhR limits disease progression by restraining neutrophil recruitment.^{14,20} In contrast, increased AhR expression in lesional T cells may largely reflect expansion of pathogenic type 17 lymphocyte populations, including Th17 cells and IL-17-producing $\gamma\delta$ T cells, which preferentially express AhR.^{21,22}

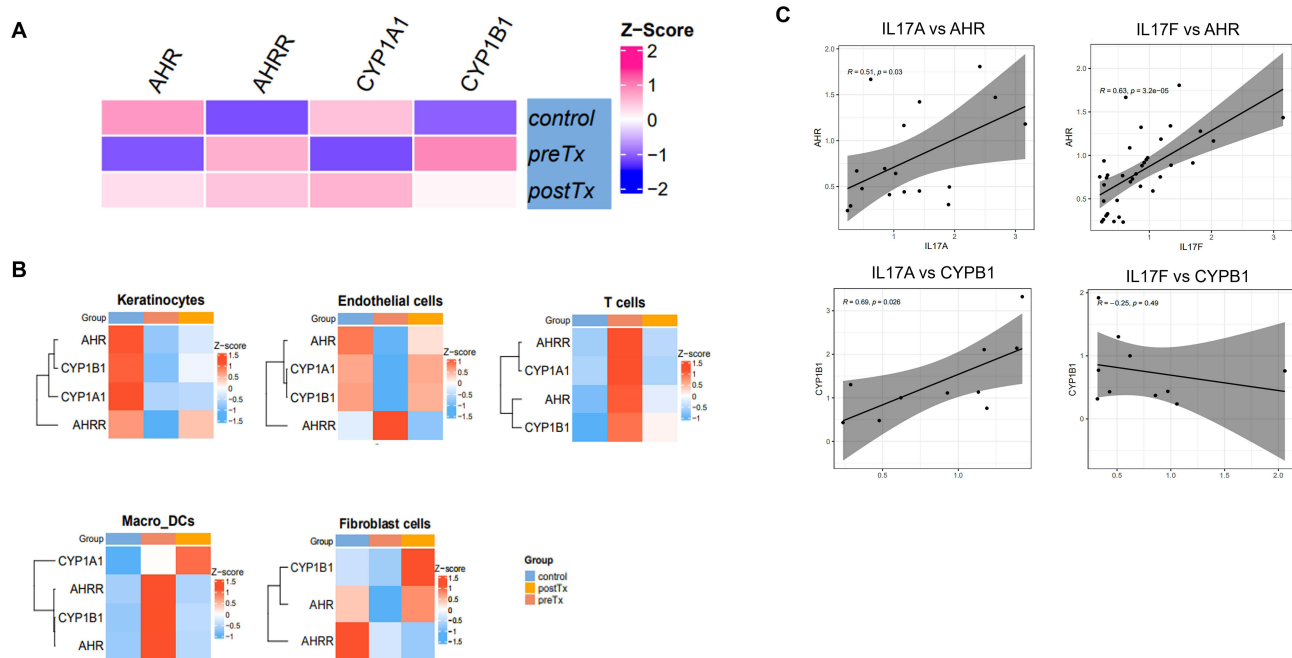


Figure 8 AhR-pathway transcriptional profiles in psoriasis skin and their relationship with IL-17 cytokines. Data derive from publicly available transcriptomic datasets (GSE183047). **(A)** Heatmap of z-score-standardized expression for AHR, AHRR, CYP1A1, and CYP1B1 in skin from healthy controls (control), psoriatic lesional skin before treatment (preTx), and lesional skin after treatment (postTx). Color scale indicates relative abundance. **(B)** Cell-type-resolved expression of the same genes in keratinocytes, endothelial cells, T cells, the macrophage/dendritic cell (Macro_DC) and fibroblast cells compartment across the three groups. Values are shown as z-scores to facilitate comparison within each gene across conditions. **(C)** Scatter plots depicting associations in preTx lesional skin between AHR, CYP1B1 expression and IL17A (left) or IL17F (right). Lines indicate fitted regressions with shaded 95% confidence intervals; the correlation coefficients and P values are annotated on the panels.

Beyond AhR, candidate mechanisms of ILA include activation of the YAP-Nrf2 axis, which suppresses inflammation in intestinal ischemia-reperfusion models,²³ and engagement of hydroxycarboxylic acid receptor 3 (HCAR3), a metabolite-responsive GPCR implicated in immune regulation and energy homeostasis.^{24,25} Differences in stimulation conditions, dose, and exposure kinetics may further bias pathway usage in keratinocytes. Further studies are warranted to define how ILA partitions between AhR-dependent immune and AhR-independent epithelial routes in psoriasis.

L. reuteri is a gut-resident probiotic that reinforces the intestinal epithelial barrier and modulates systemic inflammation. It increases tight-junction expression and reduces paracellular permeability in enterotoxigenic *Escherichia coli*-challenged epithelia,²⁶ and in DSS-induced colitis, *L. reuteri* lowers clinical scores and limits bacterial translocation to mesenteric lymph nodes.²⁶ Within *Lactobacillus* consortia, it decreases endotoxemia, autoantibody production, and renal injury in lupus-prone mice.²⁷ In psoriasis models, enrichment or supplementation with *L. reuteri* protects against IMQ-induced PsD, reducing Th17 cells, increasing IL-10, and improving skin lesions.¹⁶ Similar protection is observed after FMT that enriches *L. reuteri* in the gut microbiota. Still, the precise mechanisms remain incompletely defined. *L. reuteri* converts dietary tryptophan to ILA via the indole-3-pyruvate pathway.⁴ Consistent with a causal *L. reuteri*-ILA -AhR axis, our data show fecal ILA inversely correlates with ear thickness and cutaneous neutrophils, supporting microbial ILA biosynthesis as a tractable lever to ameliorate psoriasiform pathology and complement direct ILA therapy. Whether *L. reuteri* exerts protection via mechanisms beyond ILA-eg., histamine-H2R signaling, antimicrobial reuterin/reutericyclin, bile-acid remodeling via FXR/TGR5, or TLR2-dependent immunomodulatory exopolysaccharides-remains to be elucidated.²⁸

We used the mouse model because studies involving gut microbiota and microbiota-derived metabolites require an intact physiological context in which intestinal absorption, systemic metabolite distribution, and downstream immune responses can be evaluated together, which cannot be fully captured by in vitro or ex vivo systems alone. Nevertheless, mouse models cannot fully recapitulate the complexity of human psoriasis or human host-microbiome interactions. Several points merit consideration. First, our mechanistic inferences rest largely on the IMQ model and ex vivo stimulation; confirmation in additional psoriasis models and in human cohorts is needed. Second, AhR dependence

was inferred pharmacologically, cell type-specific genetics (eg., AhR deletion in keratinocytes or T cells) would strengthen causality. Third, the probiotic arm used a single *L. reuteri* strain; because ILA yield is strain- and substrate-dependent, we did not perform strain-resolved genomics, colonization quantification, or dietary Trp control, and other *L. reuteri* effectors were not excluded. More broadly, the gut microbiome represents an extremely complex immunologic ecosystem, and our study interrogates only a small part of this network. Multiple unmeasured factors, including environmental exposures, dietary patterns, disease background, and patient heterogeneity, may confound or modify the observed effects. Accordingly, our findings should be interpreted as supporting a plausible *L. reuteri*-ILA-AhR axis that warrants further validation across additional models of psoriasis and other autoimmune diseases, and human cohorts.

Future studies should also investigate whether ILA modulates intestinal barrier function and gut mucosal immunity, and whether such changes contribute to psoriasis through a gut-skin axis mechanism. In addition, given the systemic nature of psoriatic disease and its overlap with comorbid inflammatory conditions, it will be important to examine whether ILA-based interventions may provide benefit beyond skin inflammation, including potential effects on psoriatic arthritis-related joint involvement and IBD-associated inflammation. These directions, together with longitudinal microbiome and metabolome profiling, controlled dietary tryptophan conditions, and validation in human cohorts, will help define the translational relevance and therapeutic scope of this pathway.

Conclusion

In conclusion, our study identifies ILA as a microbiota-derived metabolite that restrains psoriasiform inflammation through AhR-dependent suppression of IL-17A-associated responses. Using IMQ-induced mouse and ex vivo models, we demonstrate that ILA ameliorates skin inflammation and provide evidence that *L. reuteri* supplementation may engage this pathway. While the broader gut microbiome-immune network remains complex and requires further validation in additional models and human cohorts, our findings support the ILA-AhR axis as a biologically relevant mechanism and a potential therapeutic avenue in psoriasis.

Abbreviations

AhR, aryl hydrocarbon receptor; AhRi, AhR inhibitor; CFU, colony-forming units; cLN, cervical lymph nodes; IAA, indole-3-acetic acid; ILA, indole-3-lactic acid; IMQ, imiquimod; IPA, indole-3-propionic acid; LC-MS/MS, liquid chromatography-tandem mass spectrometry; MFI, mean fluorescence intensity; PBS, phosphate-buffered saline; PsD, psoriasiform dermatitis; PSI, Psoriasis Severity Index (study-specific clinical score); RT-qPCR, reverse transcription quantitative PCR; TFI, total fluorescence intensity (sum signal across a gated population); Trp, tryptophan.

Data Sharing Statement

The datasets used or analysed during the current study are available from the corresponding author on reasonable request.

Acknowledgments

Zhen Meng and Jieru Ren are co-first authors for this study. This work was supported by Guangzhou Municipal–University (Institute)–Enterprise Joint Funding Program [grant number 2025A03J3773], the National Natural Science Foundation of China [grant number 82203906], Guangdong Basic and Applied Basic Research Foundation [Grant Number 2022A1515111157], Guangzhou Science and Technology Program Project [Grant Number 2025B03J0041].

Author Contributions

All authors made a significant contribution to the work reported, whether that is in the conception, study design, execution, acquisition of data, analysis and interpretation, or in all these areas; took part in drafting, revising or critically reviewing the article; gave final approval of the version to be published; have agreed on the journal to which the article has been submitted; and agree to be accountable for all aspects of the work.

Disclosure

The authors report no conflicts of interest in this work.

References

- Blauvelt A, Chiricozzi A. The immunologic role of IL-17 in psoriasis and psoriatic arthritis pathogenesis. *Clin Rev Allergy Immunol.* 2018;55(3):379–390. doi:10.1007/s12016-018-8702-3
- Krueger JG, Wharton KA, Schlitt T, et al. IL-17A inhibition by secukinumab induces early clinical, histopathologic, and molecular resolution of psoriasis. *J Allergy Clin Immunol.* 2019;144(3):750–763. doi:10.1016/j.jaci.2019.04.029
- Lai Y, Wu X, Chao E, et al. Impact of gut bacterial metabolites on psoriasis and psoriatic arthritis: current status and future perspectives. *J Invest Dermatol.* 2023;143(9):1657–1666. doi:10.1016/j.jid.2023.05.012
- Roager HM, Licht TR. Microbial tryptophan catabolites in health and disease. *Nat Commun.* 2018;9(1):3294. doi:10.1038/s41467-018-05470-4
- Pernomian L, Duarte-Silva M, de Barros Cardoso CR. The aryl hydrocarbon receptor (AHR) as a potential target for the control of intestinal inflammation: insights from an immune and bacteria sensor receptor. *Clin Rev Allergy Immunol.* 2020;59(3):382–390. doi:10.1007/s12016-020-08789-3
- Scott SA, Fu J, Chang PV. Microbial tryptophan metabolites regulate gut barrier function via the aryl hydrocarbon receptor. *Proc Natl Acad Sci USA.* 2020;117(32):19376–19387. doi:10.1073/pnas.2000047117
- Lamas B, Richard ML, Leducq V, et al. CARD9 impacts colitis by altering gut microbiota metabolism of tryptophan into aryl hydrocarbon receptor ligands. *Nat Med.* 2016;22(6):598–605. doi:10.1038/nm.4102
- Wang G, Fan Y, Zhang G, et al. Microbiota-derived indoles alleviate intestinal inflammation and modulate microbiome by microbial cross-feeding. *Microbiome.* 2024;12(1):59. doi:10.1186/s40168-024-01750-y
- Xia Y, Liu C, Li R, et al. Lactobacillus-derived indole-3-lactic acid ameliorates colitis in cesarean-born offspring via activation of aryl hydrocarbon receptor. *iScience.* 2023;26(11):108279. doi:10.1016/j.isci.2023.108279
- Cervantes-Barragan L, Chai JN, Tianero MD, et al. Lactobacillus reuteri induces gut intraepithelial CD4(+)/CD8alphaalpha(+) T cells. *Science.* 2017;357(6353):806–810. doi:10.1126/science.aah5825
- van der Fits L, Mourits S, Voerman JS, et al. Imiquimod-induced psoriasis-like skin inflammation in mice is mediated via the IL-23/IL-17 axis. *J Immunol.* 2009;182(9):5836–5845. doi:10.4049/jimmunol.0802999
- Shi Z, Wu X, Wu CY, et al. Bile acids improve psoriasiform dermatitis through inhibition of IL-17A expression and CCL20-CCR6-mediated trafficking of T cells. *J Invest Dermatol.* 2022;142(5):1381–1390.e11. doi:10.1016/j.jid.2021.10.027
- Chiricozzi A, Guttman-Yassky E, Suarez-Farinas M, et al. Integrative responses to IL-17 and TNF-alpha in human keratinocytes account for key inflammatory pathogenic circuits in psoriasis. *J Invest Dermatol.* 2011;131(3):677–687. doi:10.1038/jid.2010.340
- Di Meglio P, Duarte JH, Ahlfors H, et al. Activation of the aryl hydrocarbon receptor dampens the severity of inflammatory skin conditions. *Immunity.* 2014;40(6):989–1001. doi:10.1016/j.immuni.2014.04.019
- Zhang Y, Cheng C, Xu Z, et al. Indole-3-lactic acid inhibits keratinocyte proliferation through the aryl hydrocarbon receptor in psoriasis. *J Dermatol.* 2025;52:1831–1839. doi:10.1111/1346-8138.17947
- Chen HL, Zeng YB, Zhang ZY, et al. Gut and cutaneous microbiome featuring abundance of Lactobacillus reuteri protected against psoriasis-like inflammation in mice. *J Inflamm Res.* 2021;14:6175–6190. doi:10.2147/JIR.S337031
- Hong EH, Hyeong J, Ahn JH, et al. Limosilactobacillus reuteri alleviates psoriasis via aryl hydrocarbon receptor-mediated regulation of Interleukin-17A. *Int Immunopharmacol.* 2026;172:116194. doi:10.1016/j.intimp.2026.116194
- Meng D, Sommella E, Salviati E, et al. Indole-3-lactic acid, a metabolite of tryptophan, secreted by Bifidobacterium longum subspecies infantis is anti-inflammatory in the immature intestine. *Pediatr Res.* 2020;88(2):209–217. doi:10.1038/s41390-019-0740-x
- Ehrlich AM, Pacheco AR, Henrick BM, et al. Indole-3-lactic acid associated with Bifidobacterium-dominated microbiota significantly decreases inflammation in intestinal epithelial cells. *BMC Microbiol.* 2020;20(1):357. doi:10.1186/s12866-020-02023-y
- Zhu Z, Chen J, Lin Y, et al. Aryl hydrocarbon receptor in cutaneous vascular endothelial cells restricts psoriasis development by negatively regulating neutrophil recruitment. *J Invest Dermatol.* 2020;140(6):1233–1243.e9. doi:10.1016/j.jid.2019.11.022
- Martin B, Hirota K, Cua DJ, Stockinger B, Veldhoen M. Interleukin-17-producing gammadelta T cells selectively expand in response to pathogen products and environmental signals. *Immunity.* 2009;31(2):321–330. doi:10.1016/j.immuni.2009.06.020
- Kimura A, Naka T, Nohara K, Fujii-Kuriyama Y, Kishimoto T. Aryl hydrocarbon receptor regulates Stat1 activation and participates in the development of Th17 cells. *Proc Natl Acad Sci USA.* 2008;105(28):9721–9726. doi:10.1073/pnas.0804231105
- Zhang FL, Chen XW, Wang YF, et al. Microbiota-derived tryptophan metabolites indole-3-lactic acid is associated with intestinal ischemia/reperfusion injury via positive regulation of YAP and Nrf2. *J Transl Med.* 2023;21(1):264. doi:10.1186/s12967-023-04109-3
- Peters A, Krumbholz P, Jager E, et al. Metabolites of lactic acid bacteria present in fermented foods are highly potent agonists of human hydroxycarboxylic acid receptor 3. *PLoS Genet.* 2019;15(5):e1008145. doi:10.1371/journal.pgen.1008145
- Laursen MF, Sakanaka M, von Burg N, et al. Roager, Bifidobacterium species associated with breastfeeding produce aromatic lactic acids in the infant gut. *Nat Microbiol.* 2021;6(11):1367–1382. doi:10.1038/s41564-021-00970-4
- Karimi S, Jonsson H, Lundh T, Roos S. Lactobacillus reuteri strains protect epithelial barrier integrity of IPEC-J2 monolayers from the detrimental effect of enterotoxigenic Escherichia coli. *Physiol Rep.* 2018;6(2):e13514. doi:10.14814/phy2.13514
- Mu Q, Zhang H, Liao X, et al. Control of lupus nephritis by changes of gut microbiota. *Microbiome.* 2017;5(1):73. doi:10.1186/s40168-017-0300-8
- Mu Q, Tavella VJ, Luo XM. Role of Lactobacillus reuteri in human health and diseases. *Front Microbiol.* 2018;9:757. doi:10.3389/fmicb.2018.00757

Psoriasis: Targets and Therapy

Dovepress
Taylor & Francis Group

Publish your work in this journal

Psoriasis: Targets and Therapy is international, peer-reviewed, open access journal focusing on psoriasis, nail psoriasis, psoriatic arthritis and related conditions, identification of therapeutic targets and the optimal use of integrated treatment interventions to achieve improved outcomes and quality of life. Visit <http://www.dovepress.com/testimonials.php> to read real quotes from published authors.

Submit your manuscript here: <http://www.dovepress.com/psoriasis-targets-and-therapy-journal>